Marginal Bottleneck Identification in Power System Considering Correlated Wind Power Prediction Errors

Bin Liu, Ke Meng, Zhao Yang Dong, and Wang Zhang

***Abstract*—This letter investigates how to identify the marginal bottleneck, which is defined as the constraint most likely to be violated with the increasing wind generation uncertainty of power system in real-time dispatch. The presented method takes the correlation of wind power prediction error (WPPE) into account, leading to an ellipsoidal formulation of wind power generation region (WGR). Based on constructed WGR, the identification procedure is formulated as a max-max-min problem, which is solved by the algorithm based on iteration linear program with the proposed method to select appropriate initial points of WPPE. Finally, two cases are tested, demonstrating the efficacy and efficiency of the procedure to identify marginal bottleneck.**

***Index Terms*—Bottleneck, elliptical distribution, hyperbolic distribution, wind power accommodation.**

I. Introduction

HIGH penetration of wind power generation (WPG) brings significant challenges to power system operation due to its uncertain nature, which drives the development of new decision-making strategies [1]. On the other hand, with a given dispatch strategy p^* in real-time dispatch, the deviation of WPG from its predicted value must be balanced by other flexible units. The balancing process can be described as seeking a feasible solution of p subject to the following constraints [2].

$$p_i = p_i^* + r_i \quad \forall i \tag{1}$$

$$\sum_i p_i + \sum_i (w_i^0 + \Delta w_i \overline{w}_i) = \sum_i d_i \tag{2}$$

$$-L_l^+ \le \sum_i \pi_{il}(p_i + \Delta w_i \overline{w}_i - d_i) \le L_l^+ \quad \forall l \tag{3}$$

$$\max\{-R_i^-, p_i^- - p_i^*\} \le r_i \le \min\{R_i^+, p_i^+ - p_i^*\} \quad \forall i \tag{4}$$

where p_i, p_i^* and r_i are the corrected, given and corrective generations of flexible unit i, respectively; w_i^0, Δw_i and $\overline{w}_i$ are the predicted generation, relative wind power prediction error (WPPE) and installed capacity of wind farm (WF) i, respectively; d_i is the active power demand at bus i; R_i^-, R_i^+, p_i^-, p_i^+ are the downward and upward ramping rates and the lower and upper generation limits of thermal unit i, respectively; π_{il} is the sensitivity of bus i to line l; and L_l^+ is the transmission limit of line l.

The above formulation implies that the realized WPG will be balanced by p while satisfying the power balance constraint (2), the transmission constraint (3) and the constraint (4) depicting the generator's capability to adjust its generation. Constraint (4) is equivalent to $r_i \in [-R_i^-, R_i^+] \bigcap [p_i^- - p_i^*, p_i^+ - p_i^*]$, where the two intervals depict the ramping capability and spinning reserves of generator i, respectively. Note that the capability of power system to cope with WPG uncertainty is determined by the given dispatch strategy p^*, and some constraints might be violated when the realized WPG deviates significantly from its predicted value.

To quantify the capability of power system corresponding to a given dispatch strategy p^*, the concept of dispatchable region (DPR) is proposed in [2], which appears to be efficient and inspiring. On the other hand, an interesting problem is which constraint will be most likely to be violated. This topic has not been commonly studied, and the pioneer work is reported in [3], which proposes to determine this constraint by projecting p^* to each boundary of DPR. The boundary with minimum distance to p^* will be the most risky bottleneck. However, the correlation of WPPE, which is an inherent nature in predicting WPG, is neglected. To bridge the gap, this letter proposes a method to identify the marginal bottleneck of power system when the correlation of WPPE is taken into account, thus making helpful complement in this research topic and providing useful information for power system operator. The method is developed based on formulating wind power generation region (WGR), which depicts the possible space that the realized WPG may fall into, by ellipsoidal convex set. The identification procedure is then formulated as a tri-level max-max-min problem. With the proposed method to generate appropriate initial points, the problem can be solved by the algorithm based on iteration linear program (ITLP). Simulations on two test systems dem-

Manuscript received: April 1, 2019; accepted: September 25, 2019. Date of CrossCheck: September 25, 2019. Date of online publication: December 4, 2019.

B. Liu (corresponding author), K. Meng, Z. Y. Dong, and W. Zhang are with the School of Electrical Engineering and Telecommunications, The University of New South Wales, Sydney 2052, Australia (e-mail: bin.liu@unsw.edu.au; ke.meng@unsw.edu.au; joe.dong@unsw.edu.au; wang.zhang@unsw.edu.au).

DOI: 10.35833/MPCE.2019.000215

onstrate the efficacy and efficiency of the proposed procedure.

II. Fitting WPPE and Definition of Marginal Bottleneck

A. Fitting WPPE

Fitting WPPE has been wildly studied in literature, where the distribution parameters will be used as known information in both power system planning and operation. Among all distribution types, multivariate Gaussian distribution (MGD) has been frequently assumed. To better fit the peak and fat tails of WPPE, other distribution types, e.g., multivariate Cauchy distribution (MCD) and multivariate Laplace distribution (MLD), are employed and discussed [4]. All these distribution types actually belong to more generalized multivariate Elliptical distribution (MED) [5], whose probability density function (PDF) can be expressed as (5) when fitting WPPE.

$$f(\Delta \boldsymbol{w}) = f_0 g((\Delta \boldsymbol{w} - \boldsymbol{\mu}_1)^{\mathrm{T}} \boldsymbol{\Sigma}_1^{-1} (\Delta \boldsymbol{w} - \boldsymbol{\mu}_1)) \tag{5}$$

where f_0 and $g(\cdot)$ are a constant and a decreasing scalar function, respectively; $\boldsymbol{\mu}_1 \in \mathbb{R}^{d\times 1}$ is the expectation of $\Delta \boldsymbol{w}$ with d being the number of WFs; and $\boldsymbol{\Sigma}_1 \in \mathbb{R}^{d\times d}$ is a positive definite matrix.

To further capture the skewness of error distribution, the multivariate Hyperbolic distribution (MHD) is proved an efficient method [6], [7]. When fitting WPPE, the PDF of MHD can be expressed as:

$$f(\Delta \boldsymbol{w}) = Q \mathrm{e}^{-\alpha\sqrt{\delta^2 + (\Delta \boldsymbol{w} - \boldsymbol{\mu}_2)^{\mathrm{T}} \boldsymbol{\Sigma}_2^{-1} (\Delta \boldsymbol{w} - \boldsymbol{\mu}_2)} + \boldsymbol{\beta}^{\mathrm{T}} (\Delta \boldsymbol{w} - \boldsymbol{\mu}_2)} \tag{6}$$

$$Q = \frac{\sqrt{\pi}\,(\alpha^2 - \boldsymbol{\beta}^{\mathrm{T}} \boldsymbol{\Sigma}_2 \boldsymbol{\beta})^{\frac{d+1}{4}}}{\sqrt{2}\,(2\pi)^{\frac{d}{2}} \delta^{\frac{d+1}{2}} K_{\frac{d+1}{2}} (\delta \sqrt{\alpha^2 - \boldsymbol{\beta}^{\mathrm{T}} \boldsymbol{\Sigma}_2 \boldsymbol{\beta}})} \tag{7}$$

where $K_{\frac{d+1}{2}}(\cdot)$ is the modified Bessel function of the third kind; and $\alpha > 0$, $\delta > 0$, $\boldsymbol{\beta} \in \mathbb{R}^{d\times 1}$, $\boldsymbol{\Sigma}_2 \in \mathbb{R}^{d\times d}$, $\boldsymbol{\mu}_2 \in \mathbb{R}^{d\times 1}$ are parameters to be fitted.

Apart from the high accuracy, another interesting characteristic of employing MHD or MED to fit WPPE is that their PDF contours are ellipsoids. Note that both (5) and (6) are the decreasing function of $\Delta \boldsymbol{w}$, WGR can be constructed by imposing a minimum requirement on the PDF value ξ, leading to:

$$W(\xi) = \{\Delta \boldsymbol{w} | f(\Delta \boldsymbol{w}) \geq \xi\} \tag{8}$$

For MED, (8) can be further expressed as:

$$W(\eta) = \{\Delta \boldsymbol{w} | (\Delta \boldsymbol{w} - \boldsymbol{a})^{\mathrm{T}} \boldsymbol{G} (\Delta \boldsymbol{w} - \boldsymbol{a}) \leq u\} \tag{9}$$

where $\boldsymbol{a} = \boldsymbol{\mu}_1$; $\boldsymbol{G} = \boldsymbol{\Sigma}_1^{-1}$; and $u = \eta = g^{-1}(\xi / f_0)$ with $g^{-1}(\cdot)$ being the inverse function of $g(\cdot)$.

For MHD, (8) leads to:

$$W(\eta) = \{\Delta \boldsymbol{w} | \alpha \sqrt{\delta^2 + (\Delta \boldsymbol{w} - \boldsymbol{\mu}_2)^{\mathrm{T}} \boldsymbol{\Sigma}_2^{-1} (\Delta \boldsymbol{w} - \boldsymbol{\mu}_2)} - \boldsymbol{\beta}^{\mathrm{T}} (\Delta \boldsymbol{w} - \boldsymbol{\mu}_2) \leq \eta\} \tag{10}$$

where $\eta = -\ln(\xi / Q)$.

For (10), it is equivalent to:

$$W(\eta) = \{\Delta \boldsymbol{w} | (\Delta \boldsymbol{w} - \boldsymbol{a}(\eta))^{\mathrm{T}} \boldsymbol{G} (\Delta \boldsymbol{w} - \boldsymbol{a}(\eta)) \leq u(\eta)\} \tag{11}$$

$$\boldsymbol{G} = \boldsymbol{\Sigma}_2^{-1} - \frac{\boldsymbol{\beta}\boldsymbol{\beta}^{\mathrm{T}}}{\alpha^2} \tag{12}$$

$$\boldsymbol{a} = \boldsymbol{G}^{-1} \left(\boldsymbol{\mu}_2^{\mathrm{T}} \boldsymbol{\Sigma}_2^{-1} - \frac{\boldsymbol{\mu}_2^{\mathrm{T}} \boldsymbol{\beta}\boldsymbol{\beta}^{\mathrm{T}} - \eta \boldsymbol{\beta}^{\mathrm{T}}}{\alpha^2} \right)^{\mathrm{T}} \tag{13}$$

$$u = \boldsymbol{a}^{\mathrm{T}} \boldsymbol{G} \boldsymbol{a} - \boldsymbol{\mu}_2^{\mathrm{T}} \boldsymbol{\Sigma}_2^{-1} \boldsymbol{\mu}_2 - \delta^2 + \frac{\eta^2 + \boldsymbol{\mu}_2^{\mathrm{T}} \boldsymbol{\beta}\boldsymbol{\beta}^{\mathrm{T}} \boldsymbol{\mu}_2 - 2\eta \boldsymbol{\beta}^{\mathrm{T}} \boldsymbol{\mu}_2}{\alpha^2} \tag{14}$$

As (9) represents the interior of an ellipsoid and (10) can be reformulated to convex quadratic form similar to (9), both (9) and (10) are convex sets. Moreover, the PDF values of the WPPEs falling on the boundary of $W(\eta)$ are identical. This is easy to understand according to the expression of $W(\eta)$. For example, for (9), all boundary points of $W(\eta)$ leads to the same value of $(\Delta \boldsymbol{w} - \boldsymbol{\mu}_1)^{\mathrm{T}} \boldsymbol{\Sigma}_1^{-1} (\Delta \boldsymbol{w} - \boldsymbol{\mu}_1)$ when η is fixed, which will result in the same PDF value of $\Delta \boldsymbol{w}$ according to (5).

B. Definition of Marginal Bottleneck

Figure 1 presents the geometrical relationship between WGR and DPR (DPR is a polytope, it will be briefly revisited in Section III-A), where $W(\eta_1)$, $W(\eta_2)$, and $W(\eta_3)$ are the three WGRs with $\eta_3 > \eta_2 > \eta_1$; $\boldsymbol{R}_{\mathrm{D}}$ is the DPR determined by p^*; and the marginal point is the intersection of $W(\eta_2)$ and $\boldsymbol{R}_{\mathrm{D}}$. Obviously, any realization of WPG scenario in $W(\eta_1)$ can be accommodated. While for $W(\eta_3)$, any WPG scenario falling in $W(\eta_3) - W(\eta_3) \cap \boldsymbol{R}_{\mathrm{D}}$ will cause constraint violation. The interesting question is which constraint will be most likely to be violated as η increases. This leads to the marginal bottleneck that results from the marginal point as shown in Fig. 1. For any sufficiently small space of area dS centered at $\Delta \boldsymbol{w}$, the probability that WPPE falls into this space is $f(\Delta \boldsymbol{w})\mathrm{d}S$. Then, for all WPPEs leading to a violated constraint, the probability that WPPE falls into the space centered at the marginal point is the highest. The purpose of this letter is to identify the marginal bottleneck. Note again that the WGR is a convex set and its covering area monotonically grows with the increasing η. The marginal bottleneck can be alternatively identified via seeking the maximum $W(\eta)$ that belongs to DPR, which will be elaborated in the following section.

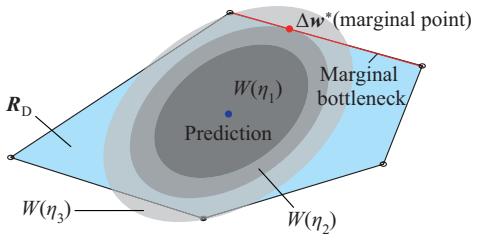

Fig. 1. Geometrical illustration of marginal bottleneck.

III. Identification of Marginal Bottleneck

A. Problem Formulation

Before introducing the proposed procedure, we first briefly revisit the method presented in [2] to construct DPR. Denoting (1) as the compact form $\boldsymbol{A}\boldsymbol{r} + \boldsymbol{B}\Delta \boldsymbol{w} \leq \boldsymbol{b}$ with $\boldsymbol{A}$, $\boldsymbol{B}$ and

$\boldsymbol{b}$ being appropriate parameters and $\boldsymbol{r}$ as the corrective variable or dispatch strategy after the realization of $\Delta\boldsymbol{w}$. The DPR can be formulated as:

$$\boldsymbol{R}_{\mathrm{D}}=\{\Delta\boldsymbol{w}|\exists\boldsymbol{r}\rightarrow\{\boldsymbol{A}\boldsymbol{r}+\boldsymbol{B}\Delta\boldsymbol{w}\le\boldsymbol{b},\forall\Delta\boldsymbol{w}\}\neq\varnothing\} \tag{15}$$

DPR has been proved to be a polytope, and can be explicitly calculated. The DPR will be used only for comparison purpose in case study.

Based on the compact formulation of (1), seeking the maximum WGR that belongs to DPR can be formulated as:

$$\max_{\eta}\ \eta \tag{16}$$

$$\text{s.t.}\quad F(\eta)=0 \tag{17}$$

$$F(\eta)=\max_{\Delta\boldsymbol{w}\in W(\eta)}\min_{\boldsymbol{z},\boldsymbol{r}}\left\{\boldsymbol{1}^{\mathrm{T}}\boldsymbol{z}|\ \boldsymbol{A}\boldsymbol{r}+\boldsymbol{B}\Delta\boldsymbol{w}-\boldsymbol{z}\le\boldsymbol{b}(\gamma),\boldsymbol{z}\ge\boldsymbol{0}\right\} \tag{18}$$

where $\boldsymbol{z}$ is the introduced slack variable; and γ is the Lagrange multiplier of the inequality constraint.

In (18), security constraints $\boldsymbol{A}\boldsymbol{r}+\boldsymbol{B}\Delta\boldsymbol{w}\le\boldsymbol{b}$ is relaxed by introducing non-negative variable $\boldsymbol{z}$. This implies if any $\Delta\boldsymbol{w}\in W(\eta)$ cannot be balanced by $\boldsymbol{r}$, $\boldsymbol{1}^{\mathrm{T}}\boldsymbol{z}$ will be positive. Therefore, constraint (17) ensures any $\Delta\boldsymbol{w}\in W(\eta)$ can be balanced by a feasible dispatch strategy $\boldsymbol{r}$. Thus, (16) is to seek the maximum $W(\eta)$, owing to which any realized $\Delta\boldsymbol{w}$ can be balanced by the flexible units of power system.

B. Algorithm

To solve (16)-(18), the inner max-min problem (18) must be solved firstly for fixed η. The approach widely used in robust optimization with polyhedral WGR is dualizing the min problem in (18) and then solving the problem by mixed-integer linear programming (MILP) or special set of order programming (SOSP) [2], [3]. However, the constructed WGR in this letter is ellipsoidal covex set with strong nonlinear nature, to apply MILP or SOSP, the minimum problem must be reformulated according to its Karush-Kuhn-Tucher (KKT) conditions, leading to:

$$\begin{aligned}F(\eta)=\max_{\Delta\boldsymbol{w}\in W(\eta),\boldsymbol{z},\boldsymbol{r},\gamma}\{&\boldsymbol{1}^{\mathrm{T}}\boldsymbol{z}|\boldsymbol{\gamma}^{\mathrm{T}}\boldsymbol{A}=\boldsymbol{0},\boldsymbol{0}\le(\boldsymbol{b}-\boldsymbol{A}\boldsymbol{r}-\\&\boldsymbol{B}\Delta\boldsymbol{w}+\boldsymbol{z})\perp\boldsymbol{\gamma}\ge\boldsymbol{0},\boldsymbol{0}\le\boldsymbol{z}\perp(\boldsymbol{1}-\boldsymbol{\gamma})\ge\boldsymbol{0}\}\end{aligned} \tag{19}$$

Note that any general complementary constraint $\boldsymbol{0}\le\boldsymbol{x}\perp\boldsymbol{y}\ge\boldsymbol{0}$ is equivalent to (20) or (21):

$$(x_i,y_i)\in SOS_1\quad\forall i \tag{20}$$

$$\begin{cases}0\le x_i\le\kappa_i M_{big}\quad\forall i\\0\le y_i\le(1-\kappa_i)M_{big}\quad\forall i\\\kappa_i\in\{0,1\}\end{cases} \tag{21}$$

where M_{big} is a big constant; and $(x_i,y_i)\in SOS_1$ implies at most one variable of x_i and y_i is non-zero, SOS_1 is the special set of order 1.

Based on (20) and (21), (19) can be further reformulated as MILP or SOSP, and solved by off-the-shelf solvers. However, the number of introduced integer or SOS_1 paired variables linearly depends on the number of constraints in (18), which relates to the security constraints in power systems. Computation inefficiency of (19) may arise even for a small-scale system, which will be demonstrated in case study later.

To tackle the computation difficulty, (18) can be alternatively solved via ITLP, where the problem is firstly reformulated as the following equivalent form.

$$F(\eta)=\max_{\Delta\boldsymbol{w}\in W(\eta),\boldsymbol{\gamma}}\left\{\boldsymbol{\gamma}^{\mathrm{T}}\boldsymbol{B}\Delta\boldsymbol{w}-\boldsymbol{\gamma}^{\mathrm{T}}\boldsymbol{b}|\boldsymbol{\gamma}^{\mathrm{T}}\boldsymbol{A}=\boldsymbol{0},\boldsymbol{0}\le\boldsymbol{\gamma}\le\boldsymbol{1}\right\} \tag{22}$$

Problem (22) is bilinear and non-convex with linear constraints. Although ITLP cannot guarantee a global solution of (22), it has been demonstrated efficient in reaching a solution of high quality with carefully selected initial points for $\boldsymbol{\gamma}$ and $\Delta\boldsymbol{w}$ [3]. For our case, ITLP can be devised as Algorithm 1.

Algorithm 1: ITLP to solve (22)

1: Initialize $\epsilon_F=10^{-6}$ and scenario set for $\Delta\boldsymbol{w}$ as $\mathcal{B}$.
2: **For** $\mathcal{B}_k\in\mathcal{B}$ **do**
3: $\Delta\boldsymbol{w}^*\leftarrow\mathcal{B}_k$, $\Delta F\leftarrow 100$
4: **while** $\Delta F>\epsilon_F$ **do**
5: $\Delta\boldsymbol{w}\leftarrow\Delta\boldsymbol{w}^*$, then solve (22) with fixed $\Delta\boldsymbol{w}$. $F_p\leftarrow F(\eta)$, and record optimum of $\boldsymbol{\gamma}$ as $\boldsymbol{\gamma}^*$.
6: $\boldsymbol{\gamma}\leftarrow\boldsymbol{\gamma}^*$, then solve (16) with fixed $\boldsymbol{\gamma}$. $F_d\leftarrow F(\eta)$, and record optimum of $\Delta\boldsymbol{w}$ as $\Delta\boldsymbol{w}^*$.
7: $\Delta F\leftarrow|F_p-F_d|$.
8: **end while**
9: $F_k\leftarrow(F_p+F_d)/2$, $\Delta\boldsymbol{w}_k^*\leftarrow\Delta\boldsymbol{w}^*$.
10: **end for**
11: Record the optimum of $\Delta\boldsymbol{w}$ in (22) as $\Delta\boldsymbol{w}_{k^*}$, where $k^*=\max_k F_k$.

Note that optimal solution of (22) must be on the boundary of $W(\eta)$, this letter proposes the following strategy to construct $\mathcal{B}$, which arises from the ideas of selecting representative scenarios in stochastic optimization and mapping arbitrary point to an ellipsoidal from a unit sphere.

A large number of initial points is generated on the surface of d dimensional unit sphere at first, and then the number of points is reduced by, e. g., successively merging the closest two points, until the number of points reaches to N. Denoting the set of selected points as $\boldsymbol{S}$, each point $\boldsymbol{y}_s\in\boldsymbol{S}$ can be mapped to the boundary of $W(\eta)$, i.e., $(\Delta\boldsymbol{w}-\boldsymbol{a})\boldsymbol{G}(\Delta\boldsymbol{w}-\boldsymbol{a})=u$, as follows [8].

$$\Delta\boldsymbol{w}_s=\boldsymbol{H}^{-1}\boldsymbol{E}^{-\frac{1}{2}}\boldsymbol{y}_s+\boldsymbol{a}\quad\forall\boldsymbol{y}_s\in\boldsymbol{S} \tag{23}$$

where $\boldsymbol{H}$ and $\boldsymbol{E}$ are from singular value decomposition (SVD) of $\boldsymbol{G}/u$, i.e., $\boldsymbol{G}=u\boldsymbol{H}^{\mathrm{T}}\boldsymbol{E}\boldsymbol{H}$ with $\boldsymbol{H}$ and $\boldsymbol{E}$ being a unitary matrix and a diagonal matrix containing all singular values of $\boldsymbol{G}/u$.

Obviously, to improve the quality of initialized points in $\mathcal{B}$, widely studied scenario-selection method in stochastic optimization can be conveniently applied.

Based on Algorithm 1, the algorithm to identify marginal bottleneck can be devised as Algorithm 2. Given a fixed η, step 2 in Algorithm 2 tests whether $W(\eta)$ is a subset of DPR. If yes, the optimal solution $\Delta\boldsymbol{w}^+$ is a boundary point of $W(\eta)$. If no, step 3-step 15 will progress to seek a boundary point falling on the section connecting $\Delta\boldsymbol{w}^0$ and $\Delta\boldsymbol{w}^+$, and η will be updated in the following step 16. The above procedure repeats until $F^*\le\epsilon_F$ is detected in step 2, implying current $W(\eta)$ is the maximum WGR belonging to DPR. The

marginal bottleneck can then be determined in step 21 via perturbing $\Delta \boldsymbol{w}$ around $\Delta \boldsymbol{w}^b$ outwardly to identify the marginal bottleneck.

Algorithm 2: identifying marginal bottleneck

1: $\eta \leftarrow 100$, $\epsilon_0 = 10^{-6}$, $\epsilon_t \leftarrow 10^{-4}$, $\epsilon_b = 10^{-2}$ and $\epsilon_F = 10^{-6}$.
2: Solve (18) by ITLP or MILP/SOSP with the given value of η. $F^* \leftarrow F(\eta)$, and record the optimum of $\Delta \boldsymbol{w}$ as $\Delta \boldsymbol{w}^+$.
3: **if** $F^* > \epsilon_F$ **then**
4: Seeking the boundary point.
5: $t_{\min} \leftarrow 0$, $t_{\max} \leftarrow 1$.
6: **while** $\Delta t = t_{\max} - t_{\min} > \epsilon_t$ **do**
7: $t \leftarrow (t_{\max} + t_{\min})/2$.
8: $\Delta \boldsymbol{w} \leftarrow t(\Delta \boldsymbol{w}^+ - \Delta \boldsymbol{w}^0)$, then solve (22) with fixed $\Delta \boldsymbol{w}$. $F_t^* \leftarrow F(\eta)$.
9: **if** $F_t^* > \epsilon_o$ **then**
10: $t_{\max} \leftarrow t$.
11: **else**
12: $t_{\min} = t$.
13: **end if**
14: **end while**
15: $\Delta \boldsymbol{w}^b \leftarrow \Delta \boldsymbol{w}$.
16: Update η as follows. For MED, $\eta \leftarrow (\Delta \boldsymbol{w}^b - \boldsymbol{\mu}_1)^{\mathrm{T}} \boldsymbol{\Sigma}_1^{-1} (\Delta \boldsymbol{w}^b - \boldsymbol{\mu}_1)$. For MHD, $\eta \leftarrow \alpha \sqrt{\delta^2 + (\Delta \boldsymbol{w}^b - \boldsymbol{\mu}_2)^{\mathrm{T}} \boldsymbol{\Sigma}_2^{-1} (\Delta \boldsymbol{w}^b - \boldsymbol{\mu}_2)} - \boldsymbol{\beta}^{\mathrm{T}} (\Delta \boldsymbol{w}^b - \boldsymbol{\mu}_2)$.
17: Go to step 2.
18: **else**
19: $\Delta \boldsymbol{w}^b \leftarrow \Delta \boldsymbol{w}^+$.
20: **end if**
21: $\Delta \boldsymbol{w} \leftarrow \Delta \boldsymbol{w}^b + \epsilon_b (\Delta \boldsymbol{w}^b - \Delta \boldsymbol{w}^0)$. Then solve inner minimization problem in (18) with fixed $\Delta \boldsymbol{w}$ to determine the marginal bottleneck.

It is noteworthy that $\Delta \boldsymbol{w}^0$ in the Algorithm 2 represents the inner point of $W(\eta)$ regardless of η. $\Delta \boldsymbol{w}^0$ equals to $\boldsymbol{\mu}_1$ for MED and for MHD, which can be determined via solving the following unconstrained optimization problem.

$$\min_{\Delta \boldsymbol{w}} f(\Delta \boldsymbol{w}) \tag{24}$$

$$f(\Delta \boldsymbol{w}) = \alpha \sqrt{\delta^2 + (\Delta \boldsymbol{w} - \boldsymbol{\mu}_2)^{\mathrm{T}} \boldsymbol{\Sigma}_2^{-1} (\Delta \boldsymbol{w} - \boldsymbol{\mu}_2)} - \boldsymbol{\beta}^{\mathrm{T}} (\Delta \boldsymbol{w} - \boldsymbol{\mu}_2) \tag{25}$$

IV. Case Study

The modified PJM-5 and IEEE-118 systems [9], where 2 and 5 WFs are connected respectively, are tested with relative WPPE fitted by MHD. The dispatch strategy p^* can also be found in [9]. The numbers of scenarios in $\mathcal{B}$ are 30 and 50 for the two systems, respectively. All algorithms are implemented on a desktop PC with Intel i7-6700 3.4 GHz CPU, 16 GB memory and solved by Gurobi 8.0.1 [10]. For comparison purpose, the SOSP to solve (22) is also implemented. Specially, the time limit for the solver when solving SOSP is set to be 3600 s to guarantee a feasible solution.

For the PJM-5 system, the high accuracy of MHD in fitting WPPE compared with MGD is demonstrated in Fig. 2, where the peak and skewness of the data can be well captured. After 3.23 s, the marginal bottleneck is identified as the transmission limit on line 5 by Algorithm 2 based on ITLP. The correctness of the result can be verified by geometrically comparing the maximum WGR and the calculated DPR as discussed in Fig. 2. Simulation results based on ITLP and SOSP for the PJM-5 bus system are compared in Table I, which shows that ITLP achieves the same accuracy as SOSP, but with much higher computation efficiency. In Table I, SOSP is solved 2 times, where the first calculation takes 190 s while the second one is terminated after the solver reaching its time limit.

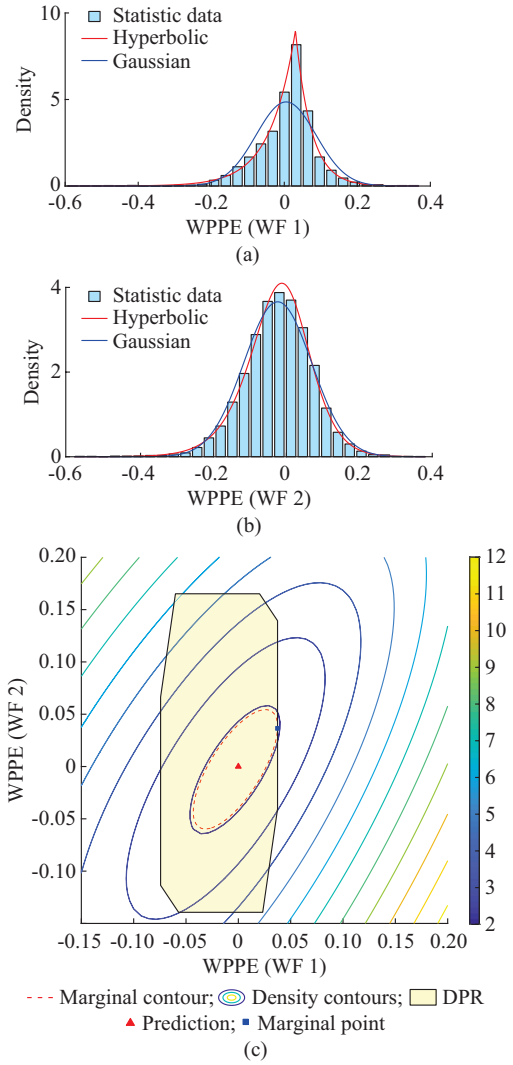

Fig. 2. Simulation results. (a) Fitting WPPE by MGD. (b) Fitting WPPE by MHD. (c) PDF density contours of WPPEs for two WFs.

TABLE I
Comparison of Algorithm 2 with ITLP and SOSP

System	Method	max(η)	Computation time (s)
PJM-5	ITLP	1.9548	3.23
PJM-5	SOSP	1.9548	>3790.00
IEEE-118	ITLP	12.6970	147.76
IEEE-118	SOSP	Failed	

To show the advantage of the proposed method being able to consider the correlation of WPPE, we change the dispatch strategy and the lower limits of thermal unit 3 to 555 MW

and 545 MW, respectively for the PJM-5 system. The formulated problem is solved again and the results are presented in Fig. 3.

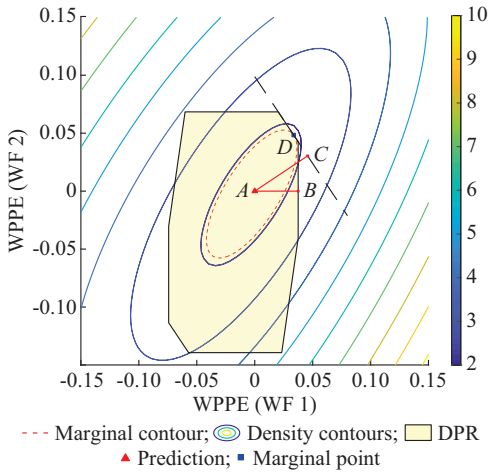

Fig. 3. Simulation results with changed parameters for thermal unit 3 for PJM-5 system.

When the correlation of WPPE is not taken into account, the boundary that has a nearest distance to the prediction point A would be the marginal bottleneck as discussed in [2], which is the transmission limit on line 5 (corresponding to boundary perpendicular to AB) for this case. By contrast, identified marginal bottleneck is the insufficient spinning reserve (corresponding to the boundary CD) when the correlation of WPPE is considered. Such results imply that identified marginal bottleneck may be quite different when the correlation of WPPE is inneglectable, thus demonstrating the advantage of the proposed method.

The marginal bottleneck for modified IEEE-118 system is successfully identified after 147.76 s, which is the ramping-up deficiency of the thermal generator located at bus 82. Simulation results based on ITLP and SOSP for IEEE-118 system are also presented in Table I where the SOSP failes to provide a feasible solution. By contrast, ITLP reports a feasible solution within reasonable time, which demonstrates the reliability of the ITLP-based algorithm.

To enhance the practicality of the proposed method, we have the following remarks.

1) Running the problem when needed. Although the interval for real-time dispatch can be as short as 5 min, the model can be calculated based on a longer period, say 15 or 30 min, or when the system is experiencing stressed demand/high-uncertain wind conditions. Under other situations, system security can be assessed by traditional $N-k$ contingency screening.

2) Employing parallel computing technique. Algorithm 1 can be implemented in parallel with different initial points, thus improving the computation efficiency of the whole calculation process.

3) Equivalating all WFs to a few virtual ones. Note that the dimension of the ellipsoidal uncertainty set is proportional to the number of WFs, to achieve a more accurate result by Algorithm 1, more initial points need to be generated, which leads to the lower computation efficiency. Through equivalating WFs that are close to each other as virtual ones, the initial points needed for Algorithm 1 can be reduced accordingly, thus improving the computation efficiency.

V. Conclusion

For WPPEs following certain practical and reasonable distribution types, the correlation of them can be effectively considered when identifying marginal bottleneck of power system. The detected bottleneck is the one with highest risk and should be paid more attention in power system dispatch. The ITLP, with the proposed method to generate initial points, is also proved to be effective and more efficient than SOSP in solving the formulated tri-level problem. Developing more efficient algorithm to solve the bilinear problem will undoubtedly benefit the practicality of the proposed procedure.

References

[1] B. Kroposki, "Integrating high levels of variable renewable energy into electric power systems," *Journal of Modern Power Systems and Clean Energy*, vol. 5, no. 6, pp. 831-837, Nov. 2017.
[2] W. Wei, F. Liu, and S. Mei, "Dispatchable region of the variable wind generation," *IEEE Transactions on Power Systems*, vol. 30, no. 5, pp. 2755-2765, Sept. 2015.
[3] W. Wei, F. Liu, and S. Mei, "Real-time dispatchability of bulk power systems with volatile renewable generations," *IEEE Transactions on Sustainable Energy*, vol. 6, no. 3, pp. 738-746, Jul. 2015.
[4] B. M. Hodge, E. Ela, and M. Milligan. (2018, Nov. 16). *The distribution of wind power forecast errors from operational systems*. [Online]. Available: https://www.nrel.gov/docs/fy15osti/52568.pdf
[5] G. Frahm, "Generalized elliptical distributions: theory and applications," Ph.D. dissertation, The University of Cologne, Cologne, Germany, 2004.
[6] D. Luthi and W. Breymann, "GHYP: a package on generalized hyperbolic distribution," Ph. D. dissertation, Institute of Data Analysis and Process Design, Zurich University of Applied Sciences, Winterthur, Switzerland, 2013.
[7] B. M. Hodge, D. Lew, M. Milligan *et al*. (2018, Oct. 16). *Wind power forecasting error distributions: an international comparison*. [Online]. Available: https://www.nrel.gov/docs/fy12osti/56130.pdf
[8] X. Zhang, *Matrix Analysis and Application*. Cambridge, USA: Cambridge University Press, 2017.
[9] *Dataset for modified PJM-5 bus and IEEE-118 bus systems*. (2018, Sept. 16)[Online]. Available: https://drive.google.com/open?id=1_npmrM63sP0CqqmgtRLVsk73CryP43G4
[10] Gurobi Optimization LLC. (2018, Oct. 10). *Gurobi optimizer reference manual*. [Online]. Available: http://www.gurobi.com

Bin Liu received the B.S degree from Wuhan University, Wuhan, China, in 2009, the M.S. degree from China Electric Power Research Institute, Beijing, China, in 2012 and the Ph.D. degree from Tsinghua University, Beijing, China, in 2015, all in electrical engineering. He is currently a research associate at The University of New South Wales, Sydney, Australia. He also worked as a research assistant at The Hong Kong Polytechnic University, Hong Kong, China in 2012 and as a power system engineer at State Grid Cooperation of China, Beijing, China, from 2015 to 2017. His research interests include energy system optimization, renewable energy integration and energy storage.

Ke Meng received the Ph.D. degree in electrical engineering from The University of Queensland, Brisbane, Australia, in 2009. He is currently a senior lecturer with the School of Electrical Engineering and Telecommunications, The University of New South Wales, Sydney, Australia. He was previously a lecturer with the School of Electrical and Information Engineering, The University of Sydney, Sydney, Australia. His research interests include pattern recognition, power system stability analysis, wind power and energy storage.

Zhao Yang Dong received the Ph. D. degree in electrical engineering from The University of Sydney, Sydney, Australia, in 1999. He is currently the SHARP professor with The University of New South Wales, Sydney, Australia, Director of ARC Research Hub for Integrated Energy Storage Solutions, Sydney, Australia, and Director of UNSW Digital Grid Futures Institute, Sydney, Australia. He was previously a professor and the Head of School of Electrical and Information Engineering, The University of Sydney, Sydney, Australia, and the Ausgrid Chair and Director of the Centre for Intelligent Electricity Networks, University of Newcastle, Callaghan, Australia. He also held industrial positions with Transend Networks (now TAS Networks), Australia. His research interest includes smart grid, power system planning, power system security, renewable energy systems, electricity market, load modelling, and computational intelligence and its application in power engineering.

Wang Zhang received the B.S. degree in electronic science and technology engineering from Beijing Institute of Technology, Beijing, China, in 2007, the M. S. degree in optoelectronics and photonics from The University of New South Wales, Sydney, Australia, in 2009 and the Ph.D. degree in electrical engineering from The University of Sydney, Sydney, Australia, in 2017. He is currently a research fellow with School of Electrical Engineering and Telecommunications, The University of New South Wales, Sydney, Australia. His research interests are power system operation, stability and control, renewable energy, and storage integration and optimization.